Journal of Membrane Science 325 (2008) 672–682

Contents lists available at ScienceDirect

Journal of Membrane Science

journal homepage: www.elsevier.com/locate/memsci

Heat and moisture transfer in application scale parallel-plates enthalpy exchangers with novel membrane materials

Li-Zhi Zhang*, Cai-Hang Liang, Li-Xia Pei

Key Laboratory of Enhanced Heat Transfer and Energy Conservation of Education Ministry, School of Chemistry and Chemical Engineering, South China University of Technology, Guangzhou 510640, China

ARTICLE INFO

Article history:
Received 26 June 2008
Received in revised form 18 August 2008
Accepted 22 August 2008
Available online 4 September 2008

Keywords:
Heat transfer
Mass transfer
Energy recovery
Parallel-plates
Membranes

ABSTRACT

Parallel-plates enthalpy exchangers are one of the most commonly encountered energy recovery devices that are used to simultaneously transfer both sensible heat and moisture between fresh air and exhaust ventilation air. For such equipments, the water vapor sorption properties of the plate materials have tremendous impacts on system performance. In this investigation, three different materials, namely, common paper, CA (cellulose acetate) membrane and a modified CA membrane) are selected as the plate materials for three enthalpy exchangers. Sorption curves and contact angles of these three materials are measured to reflect their hydrophilicity. The steady-state sensible and latent effectiveness of the three exchangers are tested in a special test rig, and the test results are compared with the model predictions. A heat and moisture transfer model for the enthalpy exchangers is proposed. The effects of the varying operating conditions like air flow rates, temperature, and humidity on the sensible and latent effectiveness are evaluated. Both the numerical and experimental results indicate that the moisture resistance through plates is co-determined by thickness, sorption slope, and sorption potential. Moisture diffusivity in various materials is in the same order. So when the plate thickness is fixed, the higher the sorption slopes are, the higher the latent performance is. Of the three exchangers, the exchanger with the modified CA membrane material has the highest performance due to small thickness, steep sorption slope, and large sorption potentials. The paper exchanger has a latent effectiveness of 0.4, while the membranes have latent effectiveness of greater than 0.7.

1. Introduction

Modern buildings and their heating, ventilating, and air-conditioning (HVAC) systems are required to be more energy efficient, while considering the ever-increasing demand for better indoor air quality, performance and environmental issues. The goal of HVAC design in buildings is to provide good comfort and air quality for occupants during a wide range of outdoor conditions. There are many researches aimed at improving the HVAC systems in buildings while reducing the energy costs and environmental impacts [1]. Some studies concentrate on control strategies and protocols like VAV (variable air volume), VRV (variable refrigerant volume) and others focus on the analysis of specific components like refrigerators, cooling coils, etc. In order for these systems to have the greatest impact, it is important for the energy needs of the building to be reduced as much as practical.

In most industrialized countries, energy consumption by HVAC sector accounts for 1/3 of the total energy consumption of the whole society. Cooling and dehumidifying fresh ventilation air constitutes 20–40% of the total energy load for HVAC in hot and humid regions. The percentage can be even higher where 100% fresh air ventilation is required [2], such as kitchen, hospital, factories. To reduce this part of energy are very crucial for the reduction of energy consumption of the whole HVAC system.

Enthalpy exchangers (or the so-called energy recovery ventilators) [2,3] could save a large fraction of energy for cooling and dehumidifying the fresh air since cool and dryness would be recovered from the exhaust stream to the fresh air in summer. With enthalpy exchangers, the efficiency of the existing HVAC systems can also be improved. The reason is that normally the fresh air is dehumidified by cooling coil through condensation followed by a re-heating process, which is very energy intensive. This part of energy can be saved if enthalpy exchangers are installed to reduce the dehumidification load. Besides energy conservation, the enthalpy exchangers have the additional benefits of ensuring sufficient fresh air supply, which is crucial for the prevention of epidemic respiratory diseases like SARS and bird flu.

* Corresponding author. Tel.: +86 20 87114268; fax: +86 20 87114268.
E-mail address: lzzhang@scut.edu.cn (L.-Z. Zhang).

0376-7388/$ – see front matter © 2008 Elsevier B.V. All rights reserved.
doi:10.1016/j.memsci.2008.08.041

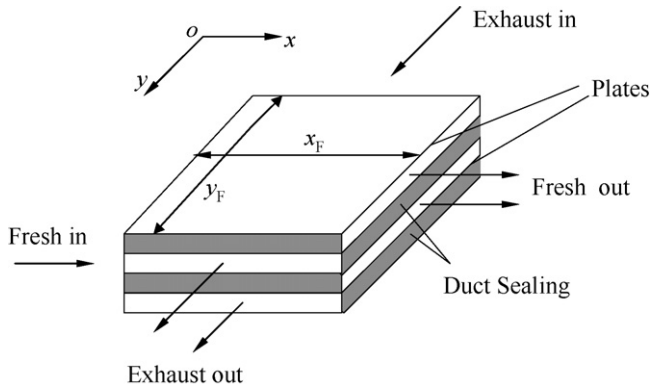

Fig. 1. Schematic of a parallel-plates enthalpy exchanger.

Parallel-plates heat mass exchangers, as depicted in Fig. 1, are the most commonly encountered enthalpy exchangers to recover both sensible heat and moisture, due to their simple structure and large packing densities. As indicated in the figure, two air streams, fresh air and exhaust air, exchange heat and moisture in a cross-flow arrangement. The reason why a cross-flow arrangement is popular is that this configuration is more convenient for duct sealing and installation. The differences between enthalpy exchangers and other air-to-air heat exchangers are that in place of metal materials, hygroscopic materials like paper and novel polymer membranes are used as the plate materials, to transfer both sensible heat and moisture simultaneously.

Though the structure seems rather simple, the practical applications of the enthalpy exchangers are rare. In fact, a membrane-based enthalpy exchanger is still in the stage of a concept. The reason is that common vapor-permeable materials like hygroscopic paper have a very low moisture transfer coefficient. Novel vapor-permeable materials like Nafion [4,5] and regenerated cellulose [6], are rather expensive. Though energy conservation has become a vogue, common consumers are still reluctant to pay for an energy recovery device with a payback time longer than 3 years. To solve these problems, recently, our laboratory has successfully developed some novel membranes for air dehumidification [7]. They are crosslinked CA (cellulose acetate) membranes and modified CA membranes. They have high vapor permeability, but are quite cheap compared to other commercially available membranes. Therefore at this stage, it is possible to build real application scale membrane-based enthalpy exchangers to further evaluate their performances.

There have been many researches on membrane related enthalpy exchangers. Kistler and Cussler [3] investigated the feasibility of using hollow fiber polymer membranes to recover heat and moisture from ventilation air. However, the pressure resistance through hollow fibers is too high to be considered commercially. Zhang and Jiang [8] studied the heat and moisture transfer in a single plate model enthalpy exchanger. The performance is high, but the details of materials are undisclosed. Niu and Zhang [2] studied the energy savings effect with a membrane-based enthalpy exchanger. They further investigated the effects of membrane materials on system performance and clarified the moisture transfer resistance [9,10]. Though they gave some insight and directions for future improvements and material selection, the studies are purely theoretical. No experimental validation was done. In summary, though there have been many studies in this area, they are purely theoretical, with little experimental work to support. To author's knowledge, studies on a practical application scale enthalpy exchanger built with parallel-plates membrane stacks have not been found in open literature. This is the objective of this research.

Fig. 2. Membrane structure.

2. Experimental work

2.1. Materials and properties

The established theory of moisture transfer in an enthalpy exchanger are governed by the following mechanisms [10]: (1) water vapor adsorbs on the plate surface in fresh air side; (2) moisture diffuses in plate thickness from fresh air side to exhaust air side; (3) water vapor desorbs from the plate surface in exhaust air side. According to this mechanism, the sorption and diffusion properties of the plate material have predominant effects on latent effectiveness. It is believed that the more hydrophilic the material is, the higher the water permeability is. To test the effects of different plate materials on the system performance, three materials: common paper, Mem1 (CA, cellulose acetate membrane) and Mem2 (a modified CA membrane) are chosen as the plate materials. They have different hydrophilicity and sorption potentials. Paper is directly bought from market. Mem1 and Mem2 are developed in our laboratory [7]. Measured thicknesses for plates are: paper, 55 μm; Mem1 and Mem2, 5 μm. Because the membranes are very thin, they are fabricated on a PP (polypropylene) net. The structure is shown in Fig. 2. The net only gives them mechanical support. Its resistance to heat and mass transfer can be neglected. The PP net has a porosity of 98% with pores larger than 1 mm and thickness around 40 μm. Its resistance is 0.4 s/m, while the membranes' resistance is larger than 14 s/m (Table 1), therefore, the PP net's resistance is negligible.

Water vapor sorption on plate materials can be expressed by the following equation:

$$\theta = \frac{W_{max}}{1 - C + (C/\phi)} \quad (1)$$

where θ is moisture uptake (kg vapor/kg dry material); ϕ is relative humidity, W_{max} represents the maximum moisture content of the membrane material (i.e., moisture uptake when $\phi = 100\%$) and C determines the shape of the curve and the type of sorption. The sorption curves can be classified into three categories: linear type, $C = 1$; type I, convex type, $C < 1$; type III, concave type, $C > 1$ [10].

Table 1
Physical properties of three plate materials

Items	Unit	Materials		
		Paper	Mem1	Mem2
W_{max}	kg/kg	0.92	0.43	2.5
C		6	11.4	8.64
D_{wm}	m^2/s	6.08E−12	1.05E−11	1.12E−11
δ	μm	55	5	5
Mean k_m	m/s	0.002	0.01	0.073
Contact angle	°	57.9	73.2	43.1
ρ_m	kg/m^3	876	760	773
λ_m	$W\,m^{-1}\,K^{-1}$	0.44	0.41	0.41

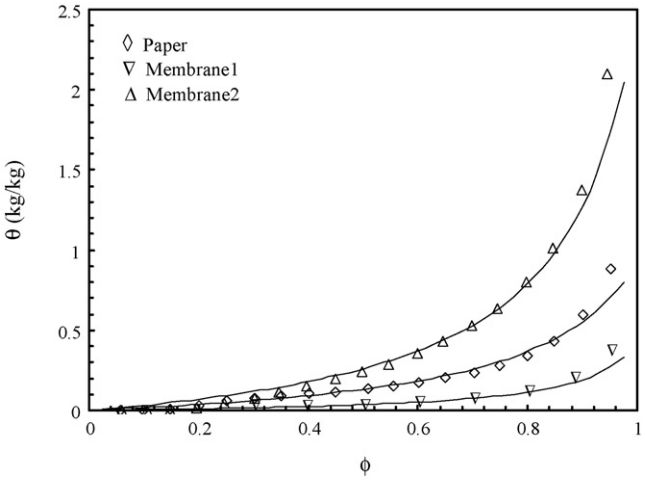

Fig. 3. Sorption curves of three materials for enthalpy exchanger.

The differentiation of Eq. (1) gives the slope of a sorption curve

$$\frac{\partial\theta}{\partial\phi} = \frac{W_{\max}C}{(1-C+(C/\phi))^2\phi^2} \tag{2}$$

It is an index of uptake change to humidity change ratio. When relative humidity changes only in a small range, the slope can be considered as linear.

The sorption curves of the three materials are measured in a vapor adsorption analyzer—Hydrosorb-1000 (Quantachrome, USA). Fig. 3 shows the three sorption curves. The discrete points are the measured data sets. The solid lines are the regressed curves by Eq. (1). The regressed coefficients in the equations are listed in Table 1. As seen, all the three materials have type III sorption curves, which implicates that the more humid the air is, the steeper the sorption slope is. Besides, the modified Mem2 has the highest sorption potential $W_{\max}$.

Generally, the higher the sorption potential is, the more hydrophilic the material is. To evaluate the material's hydrophilicity, contact angles between water droplets and plate surface are measured by a Contact Angle Analyzer (OCA20, Dataphysics, Germany). Fig. 4 is a graph showing the measurement of contact angle between distilled water and paper surface. The mean value indicated is 57.9°. The contact angles of other two materials are also measured and are listed together in Table 1. As seen, the higher

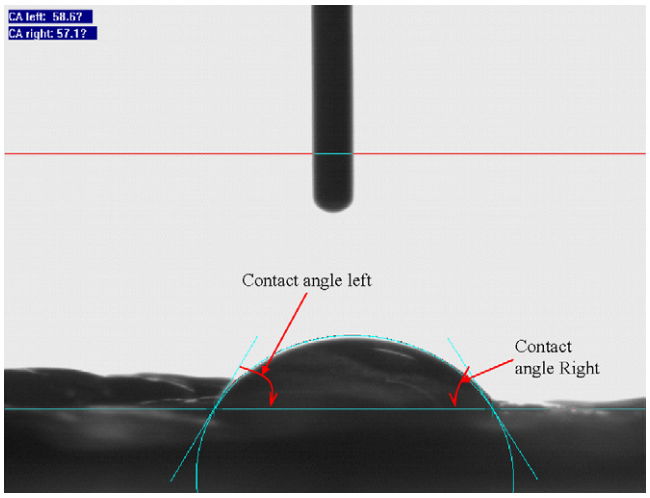

Fig. 4. Contact angle between water droplet and paper surface.

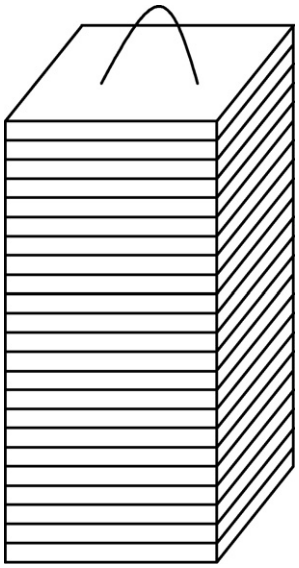

Fig. 5. Structure of the exchanger comprised of parallel-plates.

the sorption potential $W_{\max}$ is, the less the contact angle is, and the more hydrophilic the material is. In Fig. 4, the contact angles between a water droplet and the membrane surface is pointed out. The left contact angle is 58.6°, and the right contact angle is 57.1°. The mean contact angle is 57.9°.

Moisture resistance r_m through a plate is expressed by [9,10]:

$$r_m = \frac{\rho_a}{\rho_m}\frac{\delta}{D_{wm}}\psi \tag{3}$$

$$\psi = \frac{10^6 e^{(-5294/T)}}{(\partial\theta/\partial\phi)} = \frac{10^6(1-C+(C/\phi))^2\phi^2}{e^{(5294/T)}W_{\max}C} \tag{4}$$

where r_m is in s/m, δ is plate thickness (m), ρ_m is plate density (kg/m^3), ρ_a is dry air density, D_{wm} is moisture diffusivity in plate (m^2/s), ψ is a dimensionless coefficient called the CMDR (coefficient of mass diffusive resistance). The parameters in Eq. (4) like temperature T and humidity ϕ are chosen as the values on plate surface in fresh air side [10].

Moisture diffusivity in plate D_{wm} (m^2/s) is estimated with a FLEC cell [11]. The scheme is based on the basic diffusion equation of

$$E = \rho_m D_{wm}\frac{\Delta\theta}{\delta} \tag{5}$$

where E is vapor permeation rates (kg s^{-1} m^{-2}), $\Delta\theta$ is the moisture uptake difference across the paper or membrane sample. For the FLEC cell, the boundary layer resistance is known. When the permeation rates are measured, the moisture diffusivity can be calculated, with the sorption curves regressed [11]. The calculated values for the three plate materials are listed in Table 1. As seen, paper has the lowest moisture diffusivity. Mem1 and Mem2 have similar diffusivity. Generally, the three plates have diffusivity of the same order. Densities and heat conductivities for the three materials are also obtained and listed in Table 1. The key properties like density and conductivity are measured in the laboratory.

2.2. Exchangers

Three parallel-plates exchangers of the same structure are assembled with the above-mentioned three kinds of plates. They are arranged with a stack of square plates, as shown in Fig. 5. The structural parameters of the exchangers are shown in Table 2. The design air flow rate is 150 m^3/h, which can be used for ventilation

Table 2
Structural parameters of the exchangers

Item	Symbol (unit)	Value
Number of channels for each flow	n	115
Channel length	x_F, y_F (mm)	185
Channel height	a (mm)	2.0
Vapor diffusivity in air	D_a (m^2/s)	2.82×10^{-5}
Heat conductivity of air	λ_a ($W\,m^{-1}\,K^{-1}$)	0.0263
Fresh in humidity	RH_{fi}	0.59
Exhaust in humidity	RH_{ei}	0.54
Fresh in temperature	T_{fi} (°C)	35
Exhaust in temperature	T_{ei} (°C)	27

for a 20-m^2 room with 3–5 occupants, based on ASHRAE ventilation standard [12]. Therefore, the exchangers are real application scale prototypes.

2.3. Test rig

The purpose of the experiment is to measure the steady-state heat and moisture transfer through the enthalpy exchangers, by the measurements of inlet and outlet temperature, humidity and air flow rates. The sensible and latent effectiveness are the performance indices.

A schematic of the test rig is shown in Fig. 6. Two parallel air ducts with a 200 m × 200 mm cross-section are assembled. Each duct is comprised of a variable speed blower, a wind tunnel, a set of nozzles, wind straighteners, electric heating coils, steam humidification tubes, temperature and humidity sensors. An exchanger shell is designed to hold the exchanger. The small converging wind tunnels produce steady, homogeneous, fully developed air flow to the exchanger. The heating power and the steam generation currents can be adjusted according to the set points temperature and humidity. After the air temperature and humidity are adjusted to the set points, the two ducts are connected to the two inlets of the exchanger shell, respectively. The exchanger shell is designed to station the exchanger and separate the cross-flowing two air streams. The exchangers can be inserted into the quadrate cavity in the center of the shell. They can be easily replaced. The whole test rig is built in a constant temperature and constant humidity room, so the inlet temperature and humidity can be controlled and maintained very well even under very hot and humid ambient weather conditions. A 10-mm thick plastic foam insulation layer is pasted on the outer surfaces of the ducts and the shells to prevent heat dissipation from the system to the surroundings. Moisture dissipation from air stream to the surroundings is negligible since the duct and shell materials are highly hydrophobic and they could adsorb little moisture. The heat loss from the system is below 0.5%, and moisture loss is less than 0.1%. Air leakage between the two air streams are controlled to within 5%.

The nominal operating conditions: fresh air inlet 35 °C and 0.021 kg/kg; exhaust air inlet 27 °C and 0.012 kg/kg. The corresponding inlet relative humidity (RH) is 59 and 54% for fresh air and exhaust air, respectively, which are also listed in Table 2. During the experiment, equal air flow rates are kept for the two ducts. Though the design air flow rates are 150 m^3/h, in the test, they are changed by variable speed blowers, to have different air velocities. Humidity, temperature, and volumetric flow rates are monitored at the inlet and outlet of the exchanger. Before and after each test, temperature and humidity sensors are calibrated with a Pt-100 temperature sensor and a chilled-mirror dew-point meter. Hot-wire anemometers that are used to measure the wind speed before and after the exchanger are compared with the air flow rates measured by nozzles. The offset is controlled to within 1% limit. Volumetric air flow rates are varied from 100 to 200 m^3/h, corresponding to frontal air velocities from 0.37 to 0.74 m/s which are typical for commercial enthalpy exchangers. Air flow under such conditions is laminar, with Reynolds numbers not exceeding 200. A digital pressure differential gauge is used to measure the pressure drop across the tested core. The uncertainties are: temperature ±0.1 °C; humidity ±2%; volumetric flow rate ±1%, pressure drop ±1%. The final uncertainty is ±4.5% for sensible and latent effectiveness. Six sensors are uniformly positioned on the inlet and outlet surfaces of the shell to have a mean value of measurements. Due to the small channels in the core, outlet air from the core is quite evenly distributed across the outlet duct cross-section. In other words, the core itself has the effect of another ideal wind straightener. Anyway, another 6 wind straighteners, which are made of plates with numerous evenly distributed small holes drilled, are installed in the ducts before and after the shell and nozzles to well distribute the wind. In addition, heat and mass balance between the fresh air and the exhaust air are checked. Their differences are controlled to be less than 0.1%. From these preparatory works, the test rig is considered to be reliable.

The measured pressure head losses for three exchangers are the same: 43 Pa.

After the measurement of mean inlet and outlet temperature and humidity, the sensible and latent effectiveness are calculated by

$$\varepsilon_s = \frac{T_{fi} - T_{fo}}{T_{fi} - T_{ei}} \tag{6}$$

$$\varepsilon_L = \frac{\omega_{fi} - \omega_{fo}}{\omega_{fi} - \omega_{ei}} \tag{7}$$

where T and ω are temperature (°C) and humidity ratio (kg moisture/kg dry air), respectively. Subscripts "f", "e", "i", "o" refer to fresh air, exhaust air, inlet and outlet, respectively. The sensible effectiveness and the latent effectiveness are the key performance indexes to evaluate an enthalpy exchanger.

Humidity ratio and relative humidity can be calculated with psychrometric charts. It is more convenient to use an approximation as [10]:

$$\frac{\phi}{\omega} = \frac{e^{5294/T}}{10^6} - 1.61\phi \tag{8}$$

3. Mathematical model

3.1. Heat and mass transfer in air streams

An unmixed steady-state heat and mass transfer model is set up. Each flow is divided into a number of mini flows in flow cross-sections. Along each mini flow, temperature and humidity vary along flow directions (x for fresh air and y for exhaust air). The two air streams, one hot and humid (fresh air), and the other cool and dry (exhaust air), exchange both sensible heat and moisture simultaneously in the exchanger in a cross-flow arrangement. Following equations are to govern the energy and mass conservations in the two air streams:

$$\frac{\partial T_f^*}{\partial x^*} = NTU_{sf}(T_{mf}^* - T_f^*) \tag{9}$$

$$\frac{\partial T_e^*}{\partial y^*} = NTU_{se}(T_{me}^* - T_e^*) \tag{10}$$

$$\frac{\partial \omega_f^*}{\partial x^*} = NTU_{Lf}(\omega_{mf}^* - \omega_f^*) \tag{11}$$

$$\frac{\partial \omega_e^*}{\partial y^*} = NTU_{Le}(\omega_{me}^* - \omega_e^*) \tag{12}$$

where x is flow direction for fresh stream and y is flow direction for exhaust stream.

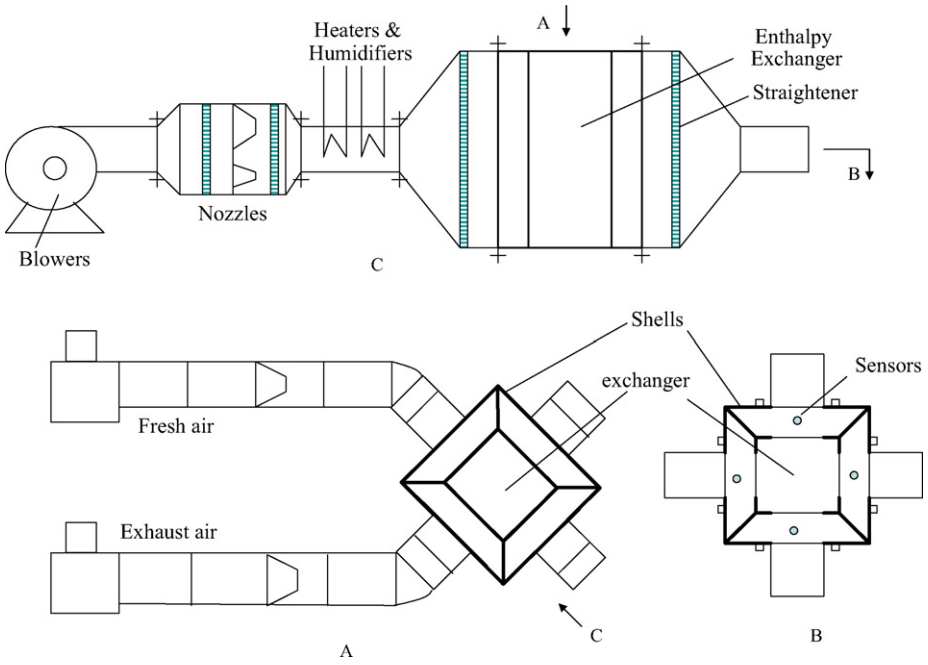

Fig. 6. Experimental set-up of the enthalpy exchanger.

The dimensionless temperature and humidity are defined by

$$T^* = \frac{T - T_{ei}}{T_{fi} - T_{ei}} \tag{13}$$

$$\omega^* = \frac{\omega - \omega_{ei}}{\omega_{fi} - \omega_{ei}} \tag{14}$$

The dimensionless coordinates are defined by

$$x^* = \frac{x}{x_F} \tag{15}$$

$$y^* = \frac{y}{y_F} \tag{16}$$

where x_F and y_F are channel lengths for fresh air and exhaust air (m), as indicated in Fig. 1. Here for square plates, $x_F = y_F$. The air side number of transfer units for heat and moisture are defined by

$$\mathrm{NTU_{sf}} = \frac{h_f A_{tot}}{G_f c_{pa}} \tag{17}$$

$$\mathrm{NTU_{se}} = \frac{h_e A_{tot}}{G_e c_{pa}} \tag{18}$$

$$\mathrm{NTU_{Lf}} = \frac{\rho_a k_f A_{tot}}{G_f} \tag{19}$$

$$\mathrm{NTU_{Le}} = \frac{\rho_a k_e A_{tot}}{G_e} \tag{20}$$

where k and h are air side convective mass transfer coefficient (m/s) and convective heat transfer coefficient (kW m^{-2} s^{-1}), respectively; G is air mass flow rate (kg/s); c_{pa} is specific heat of air (kJ kg^{-1} K^{-1}). Subscripts "mf" refers to plate surface in fresh side, and "me" refers to plate surface in exhaust side; A_{tot} is total transfer area of plates for each stream (m^2), as calculated by

$$A_{tot} = n x_F y_F \tag{21}$$

Convective heat transfer coefficient and mass transfer coefficient can be calculated by

$$Nu = \frac{hD_h}{\lambda_a} \tag{22}$$

$$Sh = \frac{kD_h}{D_a} \tag{23}$$

where D_a is vapor diffusivity in air (m^2/s), D_h is the hydrodynamic diameter (m), which is approximately equal to $(2a)$ in this structure. For parallel-plates channels, the fully developed Nusselt number is 7.54 [13]. Sherwood numbers can be calculated from Nusselt numbers by Chilton–Colburn heat mass analogy as [10,14,15]:

$$Sh = Nu\, Le^{-1/3} \tag{24}$$

where Le is commonly called the Lewis number. For ventilation air and vapor mixture, which is always near atmospheric states, the Lewis number varies in the range of 1.19–1.22.

3.2. Heat and mass transfer through plates

Heat conduction through the plate is in equilibrium with the convective heat transfer on both sides. The equilibrium can be expressed by

$$h_f(T_f^* - T_{mf}^*) = \frac{\lambda_m}{\delta}(T_{mf}^* - T_{me}^*) \tag{25}$$

$$h_e(T_e^* - T_{me}^*) = -\frac{\lambda_m}{\delta}(T_{mf}^* - T_{me}^*) \tag{26}$$

where λ_m is heat conductivity of plate (kW m^{-1} K^{-1}).

Moisture diffusion through the plate is in equilibrium with the convective mass transfer on two surfaces. The equations can be expressed by

$$\rho_a k_f(\omega_f - \omega_{mf}) = \frac{\rho_m D_{wm}}{\delta}(\theta_{mf} - \theta_{me}) \tag{27}$$

$$\rho_a k_e(\omega_e - \omega_{me}) = -\frac{\rho_m D_{wm}}{\delta}(\theta_{mf} - \theta_{me}) \tag{28}$$

Moisture uptake in plate and humidity ratio in air can be related together with sorption curve Eq. (1) and psychrometric Eq. (8). Further, considering the expression of membrane moisture transfer

resistance Eq. (3), above two equations can be re-written as

$$k_f(\omega_f - \omega_{mf}) = \frac{\omega_{mf} - \omega_{me}}{r_m} \quad (29)$$

$$k_e(\omega_e - \omega_{me}) = -\frac{\omega_{mf} - \omega_{me}}{r_m} \quad (30)$$

Thus, the driving force becomes humidity ratio on both sides of the equations.

Moisture emission rate through the plate from the fresh air to the exhaust air

$$E = \frac{\rho_a(\omega_{mf} - \omega_{me})}{r_m} \quad (31)$$

3.3. Boundary conditions

Fresh:

$$T_f^* |= 1 \quad (32)$$

$$\omega_f^* \Big| = 1 \quad (33)$$

Exhaust:

$$T_e^* |= 0 \quad (34)$$

$$\omega_e^* \Big| = 0 \quad (35)$$

4. Results and discussion

4.1. Solution procedure

A finite difference technique is used to discrete the partial differential equations developed for the air streams. The calculating domain is divided into a number of discrete nodes. Each node represents a control volume. The number of calculating node is 50 in *x*-direction. An upstream differencing scheme is used for two air streams. The two air streams and the plate are closely coupled. Heat transfer and mass transfer are also related to each other. Therefore iterative techniques are needed to solve these equations. A description of the iterative procedure is as follows:

(a) Assume initial temperature and humidity fields in the two streams.
(b) Calculate the temperature and humidity values on membrane surfaces by Eq. (25) through Eq. (30).
(c) Taking the current values of temperature and humidity on membrane surfaces as the default values, calculate the temperature and humidity profiles in two air streams by solving Eq. (9) through Eq. (12).
(d) Go to (c), until the old values and the newly calculated values of temperature and humidity at all calculating nodes are converged.

After these procedures, all the governing equations are solved simultaneously. To assure the accuracy of the results presented, numerical tests were performed for the duct to determine the effects of the grid size. It indicates that 50 grids are adequate (less than 0.1% difference compared with 90 grids). The final numerical uncertainty is 0.1%.

When the temperature and humidity fields in the exchanger are calculated, the sensible and latent effectiveness are calculated using mean outlet values, from Eqs. (6) and (7). These are the numerically obtained data. Otherwise if the measured outlet values are used in Eqs. (6) and (7), the sensible and latent effectiveness are the test data. In this study, both the experimental data and the numerical data are provided simultaneously for the analysis of performance.

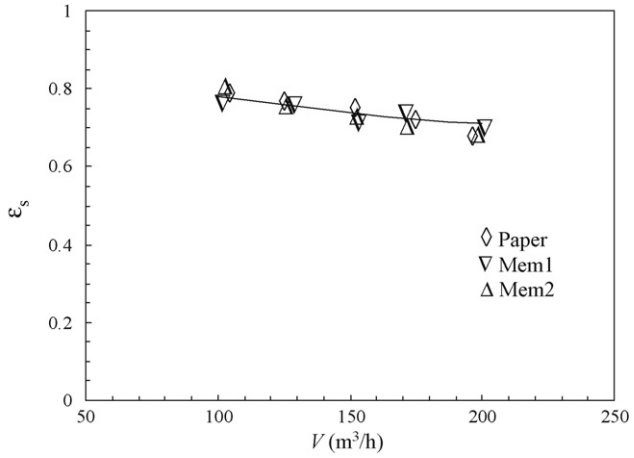

Fig. 7. Variations of sensible effectiveness with volumetric air flow rates.

4.2. Performance analysis

4.2.1. Effects of air flow rates

Due to the small plate thickness, nearly all the sensible heat resistance is in air side. Plate material has negligible influences on sensible heat transfer. Therefore, three exchangers have the same sensible effectiveness under the same operating conditions. The sensible effectiveness of the three exchangers under various volumetric air flow rates are plotted in Fig. 7. The data sets for all three materials are plotted. As seen, they are almost the same. In this figure and the following, the measured data are demonstrated by discrete symbols. The calculated data are plotted by solid lines. As seen, the predicted values and the measured values are in good agreement. The higher the volumetric air flow rates are, the less the sensible effectiveness is. Generally, the sensible effectiveness is rather high. In fact, the sensible effectiveness is from 0.8 to 0.6, showing sufficient heat transfer between the fresh air and the exhaust air. In other words, even with the common paper as the heat transfer media, the enthalpy exchanger has sufficiently high sensible performance.

In hot and humid regions, moisture recovery is more important than sensible heat recovery. For instance in summer in south China, latent load from ventilation fresh air is 2.8 times higher than sensible load. Therefore latent effectiveness of an enthalpy exchanger is the key factor for practical applications. The latent effectiveness of the three exchangers under various volumetric

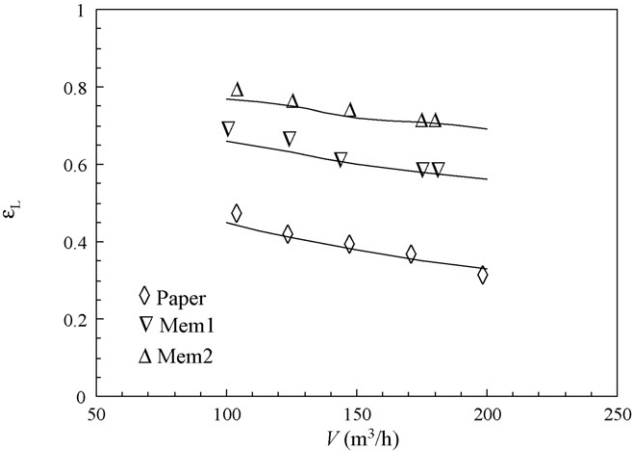

Fig. 8. Variations of latent effectiveness with volumetric air flow rates.

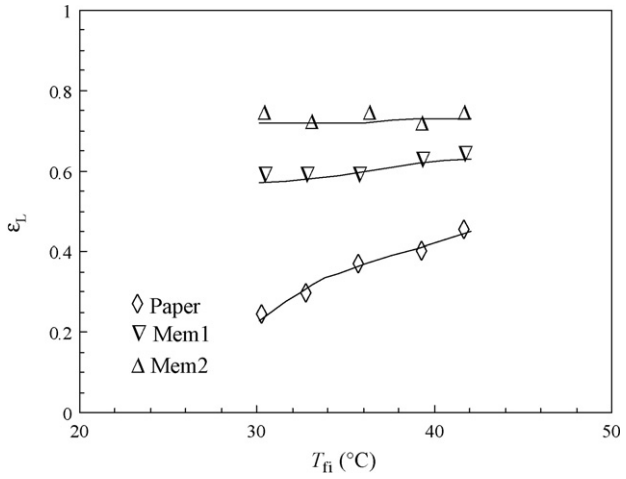

Fig. 9. Variations of latent effectiveness with fresh air temperature.

air flow rates are plotted in Fig. 8. As seen, contrary to sensible effectiveness, the latent effectiveness is quite different for three exchangers. The paper exchanger has the lowest latent effectiveness. The Mem2 exchanger has the highest effectiveness. The two membrane exchangers have latent effectiveness 60% higher than the paper exchanger. The reason lies in several factors: (1) the membranes only have 10% paper thickness; (2) the moisture diffusivities in membrane are 70% higher than in paper; (3) maximum moisture uptake in Mem3 is 1.7 times higher than in paper. All these factors contribute to the fact that Mem3 has a satisfactory latent effectiveness of 0.7, while the paper exchanger only has a latent effectiveness of 0.4. The reason why different plate materials have such different results is that the plate accounts for a large portion of the total moisture resistance.

4.2.2. *Effects of outdoor conditions*

Since outdoor temperature and humidity change from time to time, the effects of outdoor ambient conditions on performance should be considered. As previously discussed, plate materials have little influence on total sensible heat resistance, therefore fresh air temperature and humidity have little influence on sensible effectiveness. On the contrary, plate has substantial effects on latent effectiveness. In the following, the fresh air temperature and humidity will be varied to evaluate their influences on latent effectiveness.

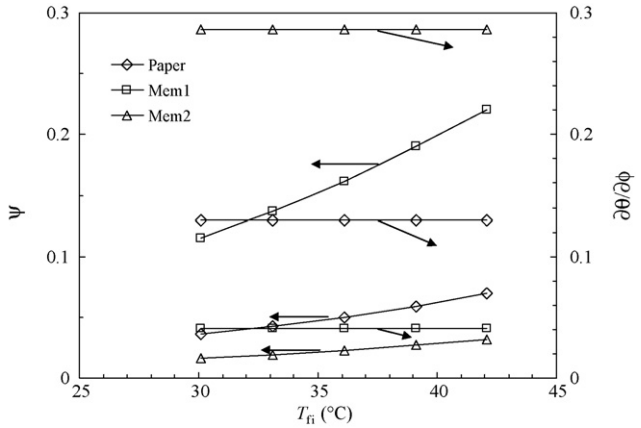

Fig. 10. Variations of coefficient of mass diffusive resistance (ψ) and sorption slope ($\partial\theta/\partial\phi$) with fresh air temperature.

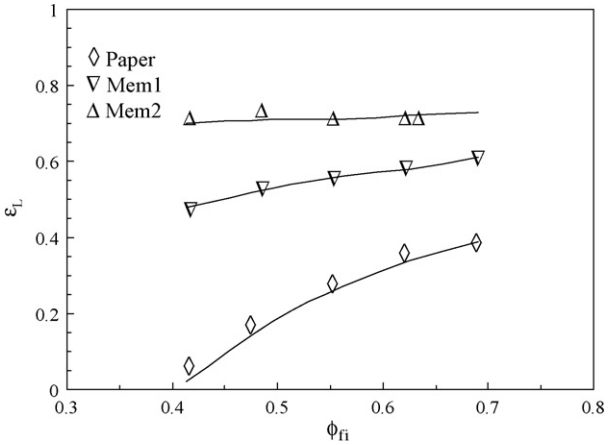

Fig. 11. Variations of latent effectiveness with fresh air relative humidity.

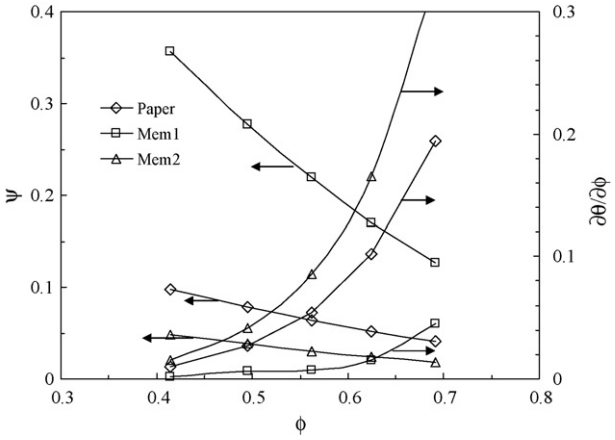

Fig. 12. Variations of coefficient of mass diffusive resistance (ψ) and sorption slope ($\partial\theta/\partial\phi$) with fresh air relative humidity.

Fig. 9 shows the variations of latent effectiveness with varying fresh air inlet temperature for the three exchangers. As seen, generally, the higher the fresh air temperature is, the higher the latent effectiveness is. The trends are the same for the three exchangers.

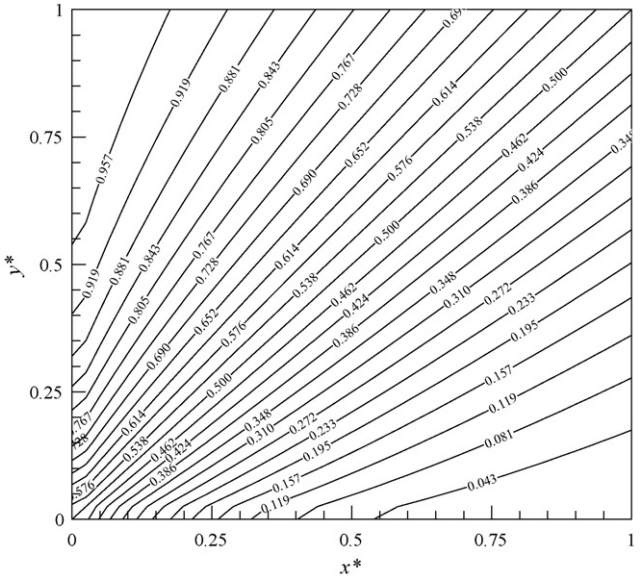

Fig. 13. Dimensionless temperature profiles on plate surface.

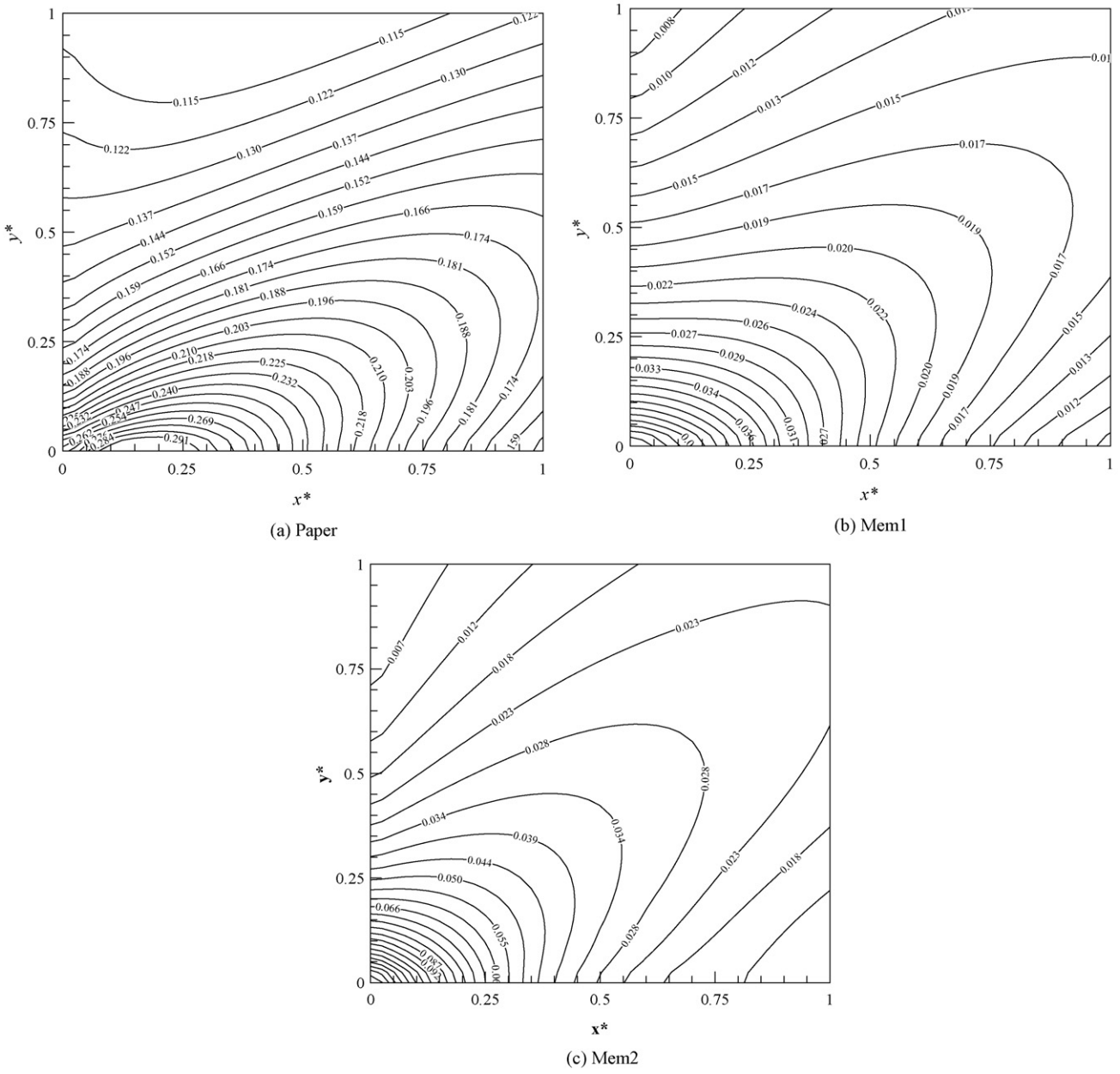

Fig. 14. Dimensionless water uptake differences between the two sides of a plate: (a) paper, (b) Mem1 and (c) Mem2.

However, the effects on the paper exchanger are the most obvious. The effects on Mem1 and Mem2 are very small. To explain this phenomenon, the variations of the coefficient of mass diffusive resistance (ψ) and sorption slope ($\partial\theta/\partial\phi$) with fresh air temperature are plotted in Fig. 10. The directions of the arrows point to respective vertical axis. The sorption slope does not change with temperature, but the coefficient of mass diffusive resistance increases with higher temperatures. This demonstrates that moisture transfer resistance increases for all the three exchangers. This increased resistance is not due to higher sorption slope ($\partial\theta/\partial\phi$), but due to the higher humidity ratio at higher temperatures. Though moisture resistance increase somewhat, fresh air side humidity ratio increase much more when the relative humidity is fixed. More moisture is adsorbed on fresh air membrane interface and permeates to exhaust side. This increased driving force is more influential than other factors. Consequently, latent effectiveness rises with temperature. The effects on paper is more obvious than other plates because paper is much thicker than membranes, therefore the driving force is the highest among the three.

Fig. 11 shows the variations of latent effectiveness with different fresh air relative humidity. As seen, latent effectiveness change much with relative humidity. The higher the relative humidity is, the higher the latent effectiveness is. As previously demonstrated, the variations of the coefficient of mass diffusive resistance (ψ) and sorption slope ($\partial\theta/\partial\phi$) with fresh air humidity are plotted in Fig. 12. As seen, for all the three materials, the higher the relative humidity is, the higher the sorption slope ($\partial\theta/\partial\phi$) is, and the less the moisture resistance through plate is. This implicates that much moisture is transferred though the plates at higher humidity. At the same time, the driving force through the plate increase with increasing relative humidity in fresh air. These two factors make the latent effectiveness increase more rapidly with increasing relative humidity. Because the paper is much thicker than membranes, and its resistance is larger, the effects of humidity on latent effec-

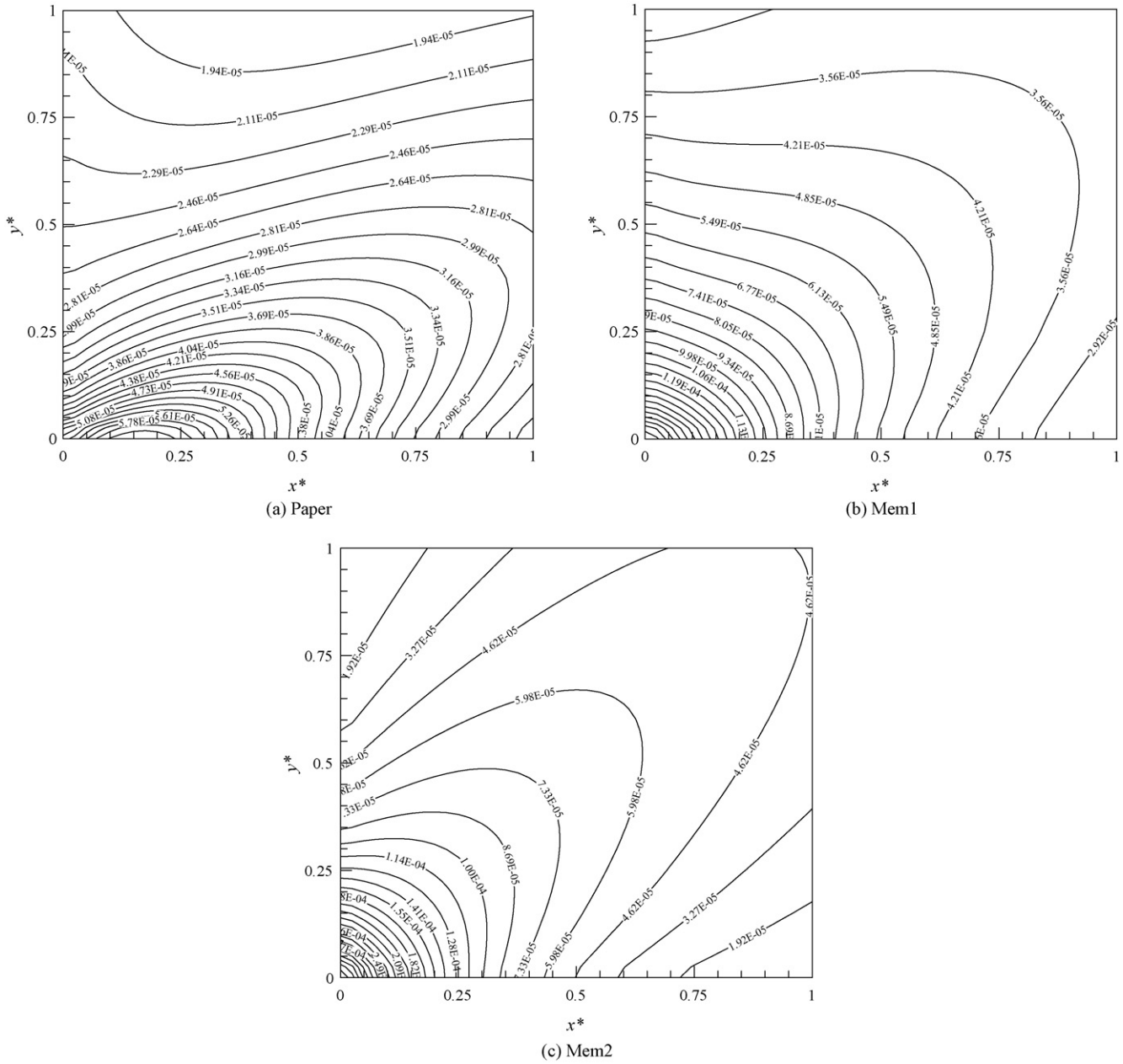

Fig. 15. Moisture emission rates across the plate (kg m^{-2} s^{-1}): (a) paper, (b) Mem1 and (c) Mem2.

tiveness for the paper exchanger are the largest among the three. Sorption slope of Mem2 is much higher than Mem1, therefore latent effectiveness of Mem2 is higher than Mem1.

4.3. Heat mass transfer through plates

The model can disclose details inside the channel that the experiment cannot. Temperature and humidity fields on plate surface are calculated under the nominal operating conditions. The dimensionless temperature fields on plate surface are shown in Fig. 13. The plate materials have little influence on sensible heat transfer. Therefore the three exchangers have the same temperature fields distribution. As seen, the temperature contours are almost parallel to the plate diagonal, meaning temperature fields in two air streams are skew-symmetric. Sensible heat resistance is the same across the plate. The local plate temperatures are almost equal to one half of the sum of local fresh air and exhaust air temperatures, indicating negligible sensible heat resistance in plate.

Moisture resistance through plate is substantial. Therefore great moisture uptake differences exist between two surfaces of a plate. Fig. 14 plots the moisture uptake differences between the two sides of three plates: paper, Mem1 and Mem2. The paper has the largest trans-plate gradients, while the Mem1 has the least gradients. The reason behind is that the paper has the largest thickness and the largest resistance and consequently the largest gradients. Mem1 and Mem2 have the same thickness and diffusivity, but sorption potential (W_{max}) and sorption slope ($\partial\theta/\partial\phi$) of Mem1 is much smaller than Mem2, as indicated in Fig. 12. As a result, trans-plate uptake difference of Mem2 is greater than Mem1, though Mem2 has a smaller resistance.

Locally distributed moisture permeation rates, calculated by Eq. (31), across the plate can also be calculated with the model. Fig. 15

shows the calculated emission rates on three plates: paper, Mem1 and Mem2. The figure discloses a phenomenon that the higher the moisture resistance through the plates is, the less the emission rates become. The order of resistance is: paper > Mem1 > Mem2 and accordingly the order of emission rates are: Mem2 > Mem1 > paper. For the membrane plates of Mem1 and Mem2, the emission rates are skew-symmetric by the plate diagonal. This indicates that moisture resistance is quite homogeneous across the plate for Mem1 and Mem2. However, for paper plate, the emission contours exhibits some degree of irregularity. The reason is that moisture resistance through paper is inhomogeneous, as a result of large thickness, great trans-plate humidity differences. The emission contours of Mem2 are the most skew-symmetric. Moisture resistance through Mem2 is the most homogeneous one. This is reasonable considering Mem2 has the least resistance and the least trans-membrane humidity differences. Sorption slopes can be considered to be a constant when relative humidity varies only in a short range.

5. Conclusions

A commercially available cheap paper and two self-made membranes are used to construct three parallel-plates enthalpy exchangers. They are application scale prototypes with a design ventilation rate of 150 m^3/h. Their performances are tested and simulated. Effects of operating conditions and material properties on sensible and latent effectiveness are investigated. Following results can be found:

(1) Due to the negligible sensible heat resistance, all three plates have the same high sensible effectiveness. Material properties and operating conditions have little influences on exchanger's sensible heat performance.
(2) Moisture transfer resistance through plates is substantial. Therefore both the material properties and operating conditions have tremendous impacts on latent effectiveness. Of the influencing factors, plate thickness is a determining factor. The thinner the plate is, the less the resistance is, and the less effects outside has. Besides thickness, material's sorption potential and sorption slope are two key factors influencing latent performance. The larger the sorption potential and sorption slope are, the higher the latent effectiveness is. From this point, materials with high hydrophilicity are the choice.
(3) The modified CA membrane of Mem2 has a very high latent effectiveness. It is also insensitive to outside operating conditions. Therefore, it has a promising future for commercialization.

Acknowledgements

This Project 50676034 is supported by National Natural Science Foundation of China. The project is also supported by the National High Technology Research and Development Program of China (863), 2008AA05Z206 and National Key Project of Scientific and Technical Supporting Programs, No. 2006BAA04B02.

Nomenclature

A_{tot}	total transfer area (m^2)
c_p	specific heat ($kJ\,kg^{-1}\,K^{-1}$)
C	constant in sorption curve
D	diffusivity (m^2/s)
D_h	hydrodynamic diameter (m)
D_{wm}	moisture diffusivity in material (m^2/s)
E	emission rate ($kg\,m^{-2}\,s^{-1}$)
G	mass flow rate (kg/s)
h	convective heat transfer coefficient ($kW\,m^{-2}\,K^{-1}$)
k	convective mass transfer coefficient (m/s)
n	number of channels for each flow
NTU	number of transfer units
Nu	Nusselt number
Sh	Sherwood number
T	temperature (K)
V	volumetric air flow rate (m^3/h)
W_{max}	maximum sorption uptake (kg/kg)
x	coordinate (m)
x_F	channel length (m)
y_F	channel length (m)
y	coordinate (m)

Greek letters

δ	thickness (μm)
ε	effectiveness
θ	moisture uptake (kg moisture/kg material)
λ	heat conductivity ($Wm^{-1}\,K^{-1}$)
ρ	density (kg/m^3)
ϕ	porosity
ϕ	relative humidity
Ψ	coefficient of mass diffusive resistance
ω	humidity ratio (kg moisture/kg air)

Superscripts

*	dimensionless

Subscripts

a	air
e	exhaust air
f	fresh air
I	inlet
L	latent
m	plates
mean	mean
o	outlet
s	sensible

References

[1] P. Talukdar, S.O. Olutmayin, O.F. Osanyintola, C.J. Simonson, An experimental data set for benchmarking 1-D, transient heat and moisture transfer models of hygroscopic building materials. Part I. Experimental facility and material property data, International Journal of Heat Mass Transfer 50 (2007) 4527–4539.
[2] L.Z. Zhang, J.L. Niu, Energy requirements for conditioning fresh air and the long-term savings with a membrane-based energy recovery ventilator in Hong Kong, Energy 26 (2) (2001) 119–135.
[3] K.R. Kistler, E.L. Cussler, Membrane modules for building ventilation, Chemical Engineering Research and Design 80 (2002) 53–64.
[4] C.R. Reineke, D.J. Moll, D. Reddy, R.A. Wessling, Water transport in ionic polymers, in: D.E. Bergheit, C.R. Martin (Eds.), Functional Polymers, Plenum Press, New York, 1989.
[5] X.H. Ye, M.D. Levan, Water transport properties of Nafion membranes. Part I. Single-tube membrane module for air drying, Journal of Membrane Science 221 (2003) 147–161.
[6] J.S. Cha, R. Li, K.K. Sirkar, Removal of water vapor and VOCs from nitrogen in a hydrophilic hollow fiber gel membrane permeator, Journal of Membrane Science 119 (1996) 139–153.
[7] L.Z. Zhang, Y.Y. Wang, C.L. Wang, H. Xiang, Synthesis and characterization of a PVA/LiCl blend membrane for air dehumidification, Journal of Membrane Science 308 (2008) 198–206.
[8] L.Z. Zhang, Y. Jiang, Heat and mass transfer in a membrane-based energy recovery ventilator, Journal of Membrane Science 163 (1999) 29–38.

[9] L.Z. Zhang, J.L. Niu, Effectiveness correlations for heat and moisture transfer processes in an enthalpy exchanger with membrane cores, ASME Journal of Heat Transfer 124 (2002) 922–929.
[10] J.L. Niu, L.Z. Zhang, Membrane-based enthalpy exchanger: material considerations and clarification of moisture resistance, Journal of Membrane Science 189 (2001) 179–191.
[11] L.Z. Zhang, Investigation of moisture transfer effectiveness through a hydrophilic polymer membrane with a field and laboratory emission cell, International Journal of Heat Mass Transfer 49 (2006) 1176–1184.
[12] ASHRAE. ANSI/ASHRAE Standard 62-2001, Ventilation for acceptable indoor air quality. Atlanta: American Society of Heating, Refrigerating and Air-Conditioning Engineers, Inc., 2001.
[13] F.P. Incropera, D.P. Dewitt, Introduction to Heat Transfer, 3rd ed., John Wiley & Sons, New York, 1996.
[14] E.L. Cussler, Diffusion-Mass Transfer in Fluid systems, Cambridge University Press, 2000.
[15] R. Taylor, R. Krishna, Multicomponent Mass Transfer, John Wiley & Sons, Inc., New York, 1993.